

## ***Supporting Information***

### **Transition-Metal Ions Intercalation Chemistry Enabled Manganese Oxides-Based Cathode with Enhanced Capacity and Cycle Life for High-Performance Aqueous Zinc-Ion Batteries**

Hongyu Zhao<sup>1,\*</sup>, Li Wang<sup>1</sup>, Meiling Li<sup>1</sup>

<sup>1</sup>School of Electronic Engineering, Lanzhou City University, Lanzhou 730000, Gansu, People's Republic of China

Corresponding author, E-mail address: [ruofan\\_1007@126.com](mailto:ruofan_1007@126.com)

#### **1. The nominal valence states calculation**

The nominal valence states of Mn of the different samples can be calculated based on the measured  $\Delta E$  in Figure 2b, which can be determined quantitatively with the following equation.<sup>1-2</sup>

$$AOS = 8.956 - 1.126 \Delta E$$

Where AOS denotes the calculated nominal valence states of Mn. The energy differences ( $\Delta E$ ) were measured with 4.63 eV, 4.98 eV, and 5.21 eV for the  $MnO_2$ ,  $MnO_2\text{-Na}$  and  $MnO_2\text{-Cu}$  samples, respectively. Accordingly, the valence states of Mn in  $MnO_2$ ,  $MnO_2\text{-Na}$ , and  $MnO_2\text{-Cu}$  are 3.74, 3.35, and 3.1, respectively.

## 2. Supplementary Figures

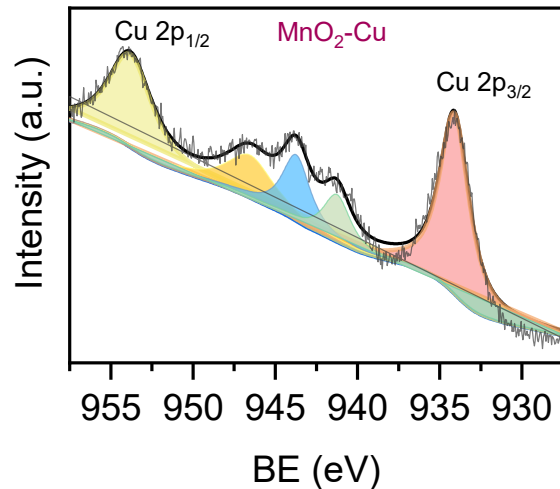


**Figure S1.** XPS core-level spectra of Cu 2p of the obtained MnO<sub>2</sub>-Cu.

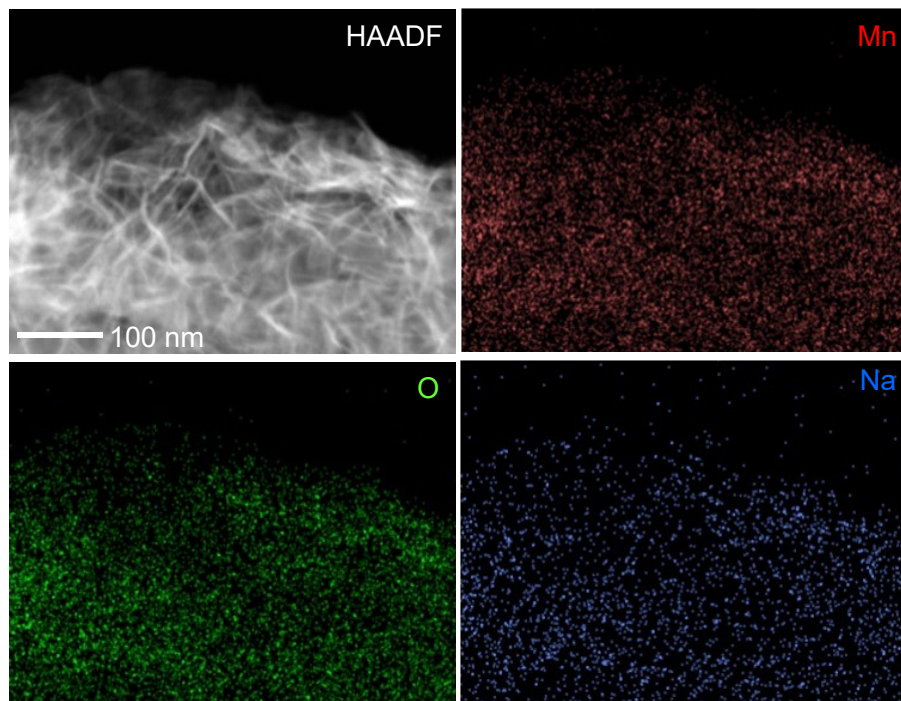


**Figure S2.** Elemental maps of the sample MnO<sub>2</sub>-Na.

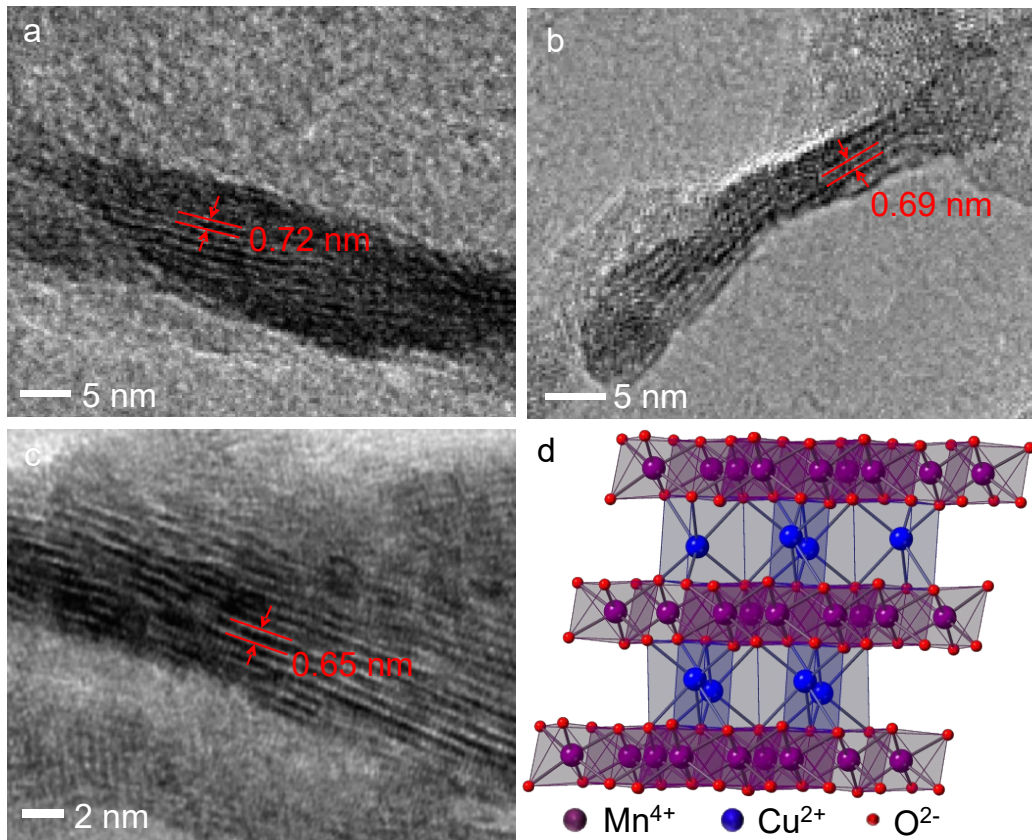


**Figure S3.** Representative TEM images with the lattice stripe view of the obtained MnO<sub>2</sub>, MnO<sub>2</sub>-Na, and MnO<sub>2</sub>-Cu. (a) MnO<sub>2</sub> with the interlayer spacing of 0.72 nm; (b) MnO<sub>2</sub>-Na with the interlayer spacing of 0.69 nm; (c) MnO<sub>2</sub>-Cu with the interlayer spacing of 0.65 nm; (d) schematic illustrating the crystal structure of MnO<sub>2</sub>-Cu with the interlayer intercalated Cu<sup>2+</sup>.

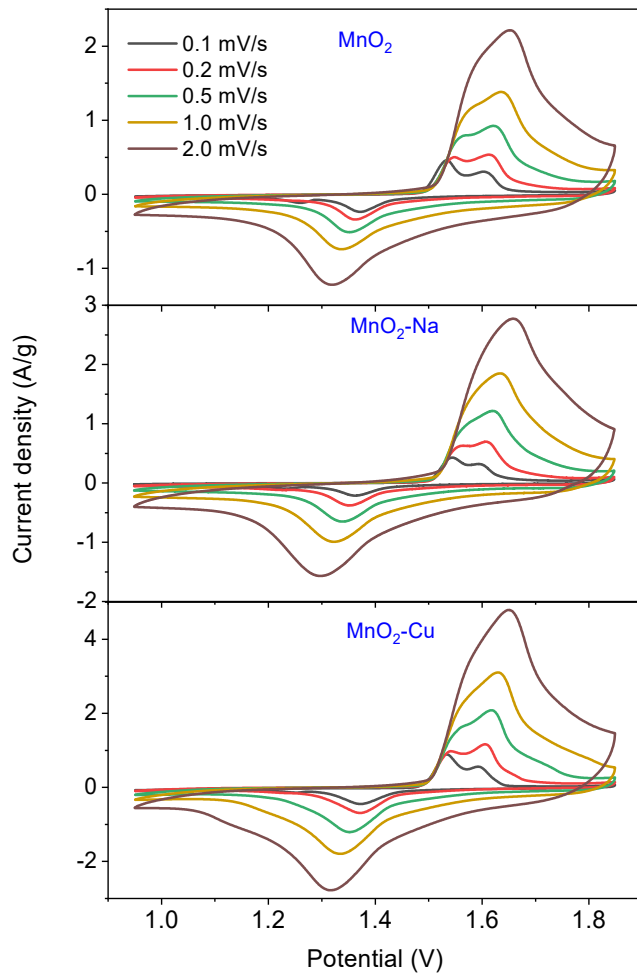


**Figure S4.** CV curves of the obtained  $\text{MnO}_2$ ,  $\text{MnO}_2\text{-Na}$ , and  $\text{MnO}_2\text{-Cu}$  electrodes were recorded at the scan rate ranging from 0.1  $\text{mV/s}$  to 2.0  $\text{mV/s}$ .

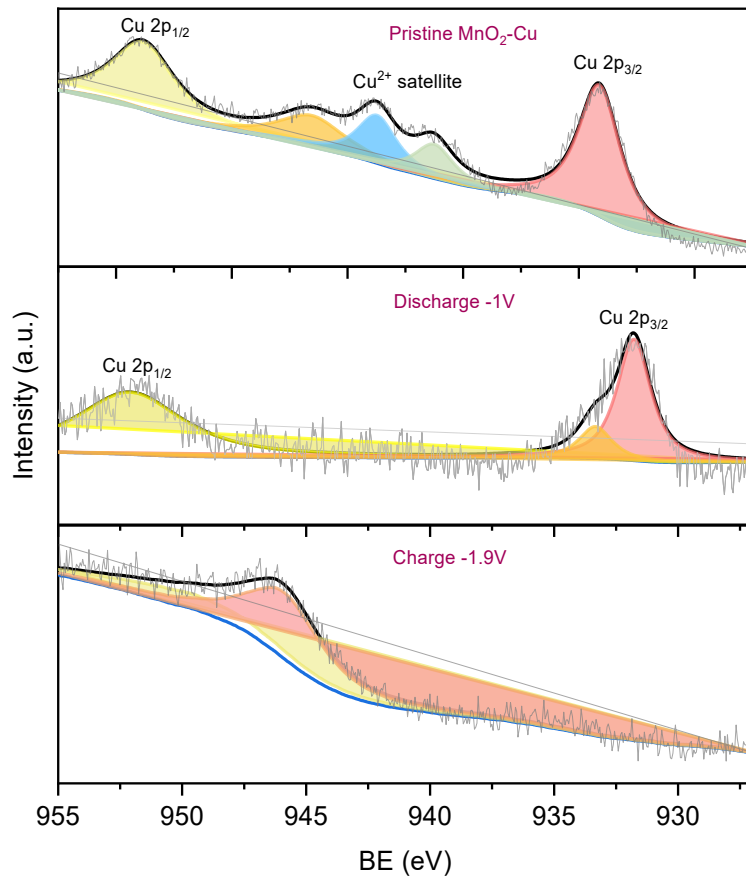


**Figure S5.** Valence states evolution of Mn in the  $\text{MnO}_2$ -Cu electrode during different charge-discharge stages.

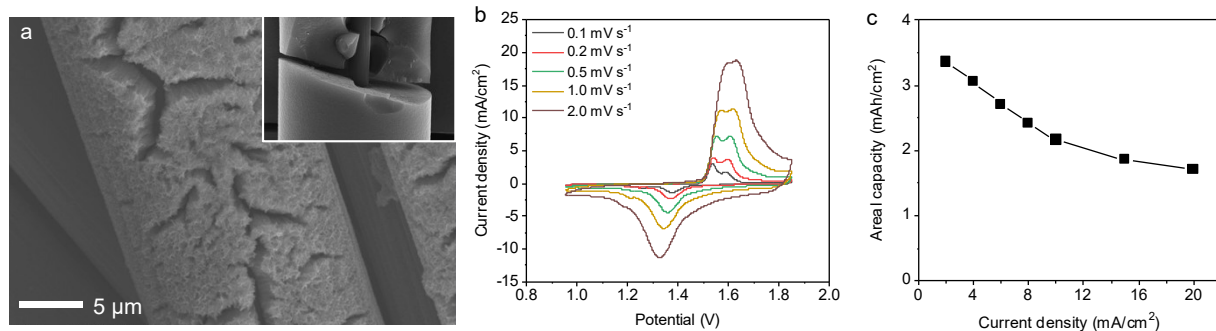


**Figure S6.** Electrochemical performance of  $\text{MnO}_2$ -Cu electrodes with high mass loading up to  $9.6 \text{ mg/cm}^2$ . (a) Typical SEM image of the  $\text{MnO}_2$ -Cu electrodes revealing the significantly thicker  $\text{MnO}_2$ -Cu materials electrodeposited on the current collector carbon cloth; (b) CV curves recorded at different scan rates ranging from  $0.1 \text{ mV/s}$  to  $2.0 \text{ mV/s}$ ; (c) Rate capability at different charge-discharge current densities.

## Reference

- 1 X. Tan, R. Liu, C. Xie and Q. Shen, *J. Power Sources*, 2018, **374**, 134-141.
- 2 A. Manceau, M. A. Marcus and S. Grangeon, *Am. Mineral.*, 2012, **97**, 816-827.